Polymer(Korea), Vol. 40, No. 6, pp. 998-1004 (2016)
http://dx.doi.org/10.7317/pk.2016.40.6.998

ISSN 0379-153X(Print)
ISSN 2234-8077(Online)

전기방사에 의한 폴리에틸렌 옥사이드와 Nitrogen으로 기능화된 박테리아 셀룰로오스 나노휘스커 복합체의 나노섬유 제조와 특성 평가

윤옥자†

중앙대학교, 물리학과, 신기능이미징연구소

(2016년 8월 9일 접수, 2016년 9월 1일 수정, 2016년 9월 4일 채택)

Preparation and Thermal Properties Evaluation of Polyethylene Oxide and Nitrogen-Functionalized Bacterial Cellulose Nanowhisker Composite Nanofibers via Electrospinning

Ok Ja Yoon†

Department of Physics, Institute of Innovative Functional Imaging, Chung-Ang University, Seoul 06974, Korea

(Received August 9, 2016; Revised September 1, 2016; Accepted September 4, 2016)

초록: 본 연구는 폴리에틸렌 옥사이드/질소기가 형성된 박테리아 셀룰로오스 나노휘스커(PEO/N-BCNWs) 복합 나노섬유를 제작하였다. PEO/N-BCNWs 복합 나노섬유는 폴리에틸렌 옥사이드 나노섬유, 폴리에틸렌 옥사이드/박테리아 셀룰로오스 나노휘스커 복합 나노섬유와 비교하여 직경이 가늘어 졌고 균일하게 형성되었음을 확인하였고, 열중량 분석으로부터 ash가 높게 남아있음을 확인하였다. 그러나 시차 주사 열량계 분석으로부터 융합점이나 결정화 온도가 농도 증가에 따라서 감소되고 있음을 확인할 수 있었다. 이러 결과들로부터 기능화된 N-BCNWs를 필러로써 복합화한 나노섬유의 열적 특성 변화를 확인할 수 있었고 바이오나 센서 등의 응용이 가능할 것으로 판단된다.

Abstract: Composite of polyethylene oxide (PEO)/nitrogen-containing bacterial cellulose nanowhiskers (N-BCNWs) were prepared using an electrospinning method and compared to electrospun PEO and composite of PEO/bacterial cellulose nanowhiskers (BCNWs). N-BCNWs were prepared by plasma treatment of BCNWs using a microwave oven, after which the presence of nitrogen-containing functional groups (2.74%) on their surface was confirmed. The diameter of the electrospun PEO/N-BCNWs was smaller than that of PEO/BCNWs composite nanofibers with the same PEO and BCNW concentrations. The weight losses, melting temperature and crystallization temperature of PEO/N-BCNWs were also lower than those of the other electrospun samples. These results show that the nitrogen-functionalized BCNWs used as a filler in the PEO polymer are suitable for application in humidity sensor and biomedical fields.

Keywords: polyethylene oxide nanofibers, nitrogen functionalization, bacterial cellulose nanowhisker, thermal properties evaluation, microwave oven.

Introduction

Polyethylene oxide (PEO) is a water soluble polymer that has been classified as an eco-friendly material because it is non-toxic, biocompatible, and biodegradable.[1] PEO is now widely applied in biomedical fields,[2-5] as an electrolyte,[6] and humidity sensor.[7] However, PEO has poor mechanical properties and is very fragile.[8,9] Previously, researchers reported that the mechanical properties of electrospun PEO with incorporated bacterial cellulose whiskers (BCWs) improved with increasing cellulose whisker concentration (0.2 and 0.4 wt%) by increasing the nanofiber diameter. Incorporation of 0.4 wt% cellulose whiskers improved the tensile modulus, tensile strength, and elongation of electrospun PEO by 193.9, 72.3 and 72.3%, respectively.[10] In addition, the incorporation of 0-20 wt% wood-based cellulose nanocrystal (CNC) into (5 and 7 wt%) led to formation of PEO/CNC composite nanofibrous mats with both homogeneous and heterogeneous microstructures due to the high PEO/CNC concentration in the mixture. The thermal and mechanical properties of heterogeneous

†To whom correspondence should be addressed.
E-mail: yokk777@cau.ac.kr

microstructures were enhanced compare to homogeneous microstructures.[11]

Bacterial cellulose (BC) has been used in various composite materials for many different applications, including as a filler in polymers,[12,13] transparent and electro active paper,[14,15] tissue engineering,[16] food industry,[17] drug delivery systems,[18] opto-electronic device,[19] and organic light emitting devices.[20] BC synthesized by *Gluconacetobacter xylium* has a high crystallinity and ultrafine structure (< 100 nm diameter),[21,22] and its mechanical properties are superior to those of cellulose extract from plants.[23] In addition, bacterial cellulose nanowhiskers (BCNWs), where the BC was treated by acid hydrolysis have been reported to have high aspect ratio and good dispersion.[24] BCNW surfaces contain carboxyl and hydroxyl groups, while nitrogen-functionalized BCNWs (N-BCNWs) have nitrogen-containing groups suitable for biomedical applications, such as enhancing cell adhesion and viability.[25] Previously, we have reported composite nanofibers made from polymers with enhanced mechanical and thermomechanical properties, as well as nitrogen or amine plasma-treated carbon materials that showed biological affinity.[26] However, the preparation of PEO/N-BCNW composite nanofibers and evaluation of their thermal properties have not yet been investigated.

In this study, we prepared N-BCNWs using plasma treatment with a microwave oven and investigated the effects of N-BCNWs embedded into electrospun PEO. Electrospun PEO, PEO/BCNWs, and PEO/N-BCNWs were fabricated by an electrospinning method. The electrospun PEO/BCNWs and PEO/N-BCNWs were classified according to the concentration of BCNWs and N-BCNWs (0.3 and 0.5 wt%, respectively) embedded in the electrospun PEO. The morphology and thermal properties such as weight loss, melting temperature (T_m), and crystallization temperature (T_c) in all sample types were compared.

Experimental

Fabrication of BCNWs and N-BCNWs. Bacterial cellulose (BC) produced by *Gluconacetobacter xylium* was purchased from the Korean Culture Center of Microorganisms (KCCM, No. 41431). The culture medium was a mixture consisting of yeast extract (Becton Dickinson and Company, Sparks, Maryland, USA), peptone (Becton Dickinson and Company, Sparks, Maryland, USA), and D-mannitol (99.0%, Samchun Pure Chemical Co., Ltd) in quantities of 0.75, 0.45, and 1.5 g, respectively. The medium was adjusted to pH 4 and autoclaved at 120 °C for 20 min. The inoculated bacterial cells were pre-cultured by the static culture method[27] for 12 h at 26 °C and the resulting BC pellicles were purified using 38 μm filter paper. A 3% bacterial cell suspension was then transferred to fresh medium (400 mL) and a film of BC pellicles was formed by growth at 26 °C for 20 days. To obtain purified BC, the bacteria in the BC pellicles were removed by boiling in a 1 M aqueous NaOH solution for 30 min. The BC had a neutral pH after several rinses with distilled water. Purified BC pellicles were put in 65 wt% sulfuric acid and stirred at about 70 °C for 2 h. BCNWs were obtained by repeated rinsing in distilled water and centrifugation at 14000 rpm for 30 min (resulting in a neutral pH). Purified BCNW powders were obtained by freeze drying. The N-BCNWs were prepared by N_2 plasma treatment of BCNWs using a microwave oven. The BCNWs were placed in a 320 mL glass lock, into which N_2 gas was injected through a gas tube. The glass lock was located in a microwave oven (LG electronics, MW-209EC, Korea) and the N_2 plasma treatment was carried out at 2450 MHz for 2 min.

Preparation of Electrospun PEO, PEO/BCNWs and PEO/N-BCNWs. BCNW and N-BCNWs (0.3 and 0.5 wt%) were mixed with deionized water (DW) and dispersed through ultrasonication for 2 h. PEO with a viscosity molecular weight (M_v) of 400000 g·mol^{-1} was purchased from Sigma Aldrich, USA. An 8 wt% PEO solution was prepared in DW and either the BCNWs or N-BCNWs were added to prepare the desired concentration (0.3 or 0.5 wt%). These solutions were homogenized using a magnetic stirrer for 5 h. The electrospinning process involved placing the prepared solutions in a 10 mL syringe with a 21G needle. The polymer solution was supplied to the needle tip by a syringe pump with a rate of 0.1 mL/h. A voltage of 13.1 kV was applied between the needle tip (anode) and a collecting plate (cathode) at a distance of 18 cm. As a result of the evaporation of the DW solvent from the polymer solution and the applied electric field, the electrospun sheets with a thickness of about 7±0.3 μm (N=5) were formed.

Characterization of Electrospun PEO, PEO/BCNWs, and PEO/N-BCNWs. The morphology and thickness of the electrospun samples were measured using field emission scanning electron microscopy (FE-SEM; JSM 7500F, JEOL Ltd., Japan). Images of BCNWs and N-BCNWs embedded in PEO nanofibers were taken using high-resolution scanning transmission electron microscopy (HR-STEM; Tecnai G^2-F30, USA). The surface chemical properties of BCNWs and N-BCNWs were investigated by X-ray photoelectron spectros-

copy (XPS; PHI Quantera-II, Japan). XPS spectra were measured using a pass energy of 20 eV with non-monochromatic Al Kα radiation (195 W) over a wide scan range (1-1000 eV). The hydrocarbon C1s peak at a binding energy of 285 eV was used as a reference for the core-level signals. Spectral analysis of the peak shape was performed by Gaussian fitting. Chemical and structural analysis of all composite nanofibers were performed with Fourier-transform infrared spectrophotometry (FTIR; Nicolet 6700, Thermo Scientific Corp., USA). The FTIR spectra were obtained by 32 scans taken a resolution of 4 cm^{-1} in frequency range of 4000-650 cm^{-1}.

Thermogravimetric analysis (TGA) was performed using a thermobalance (TG/DTA 7300, Seiko Instruments) of 8.8 mg at a heating rate of 10 °C/min under a flow of nitrogen gas. Differential scanning calorimetry (DSC; DSC 6100, Seiko Instruments) was performed on a sample with an initial weight of about 6.8 mg under a flow of nitrogen at a heating rate of 5 °C/min. The analysis involved increasing the temperature from 23 to 300 °C followed by continuous cooling to 23 °C. TGA and DSC measurements were performed in duplicate.

Results and Discussion

Morphology and Characteristics of BCNWs and N-BCNWs. An SEM image of some BCNWs showing the microcrystalline structure (diameter: <100 nm, aspect ratio: 58.18±12.05 (N=20)) consisting of nanofibers and microfiber bundles is shown in Figure 1(a). After N_2 plasma treatment (Figure 1(b)), no morphological changes or surface damage was observed on the N-BCNWs compared to the BCNWs. The C1s, O1s and N1s peaks of the BCNW and N-BCNW samples identified with XPS are shown in Figure 2(a-e) and the atomic concentration of C, O, and N on each sample surfaces are shown in Table 1. The C1s regions of the BCNWs consist of four components; at 284.3 eV (C=C), 285.3 eV (C-C and C-H), 287.3 eV (O-C-O), and 288.2 eV (O-C=O). The O1s peak from the BCNWs consisted of three contributions; at 530.8 eV (C=O), 532.3 eV (C-O), and 533.9 eV (O=C-O/O-C=O).[25,28] The C1s regions of the N-BCNWs appeared at 284.1, 285.7, 286.9 and 287.2 eV. The peaks of at 286.9 eV confirmed a slight shift with respect to that of BCNWs (at 288.2 eV). The O1s region of N-BCNWs was similar as that of BCNWs with contributions at 530.7, 532.2 and 533.3 eV. The oxygen-carbon ratio (O/C) on the surface of N-BCNWs increased with 137% compare to that of BCNWs.[29] The nitrogen content of the N-BCNWs was measured as 2.74% and the N1s spectrum showed a peak with 399.5 eV (pyridine region), consistent with Pertile *et al*., who previously reported that the N1s region decomposed into only one peak with a binding energy of 400.3 eV.[25] The above XPS data clearly confirmed the formation of nitrogen-containing functional groups on the surface of the BCNWs as a result of the plasma treatment.

Morphology of Electrospun PEO, PEO/BCNWs, and PEO/N-BCNWs. The morphology of the electrospun PEO, PEO/BCNWs, and PEO/N-BCNWs as a function of the BCNWs and N-BCNWs concentration is shown in Figure 3.

The diameter of the PEO nanofibers shown in Figure 3(a) were 0.57±0.2 μm (N=20), whereas those of the electrospun

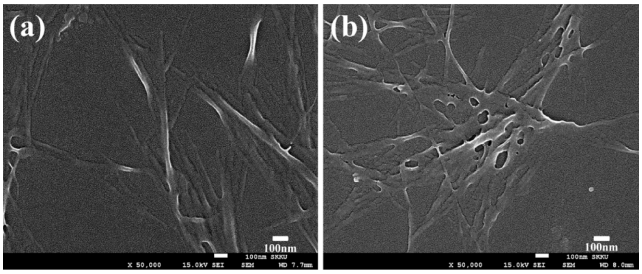

Figure 1. Morphology of (a) BCNWs; (b) N-BCNWs.

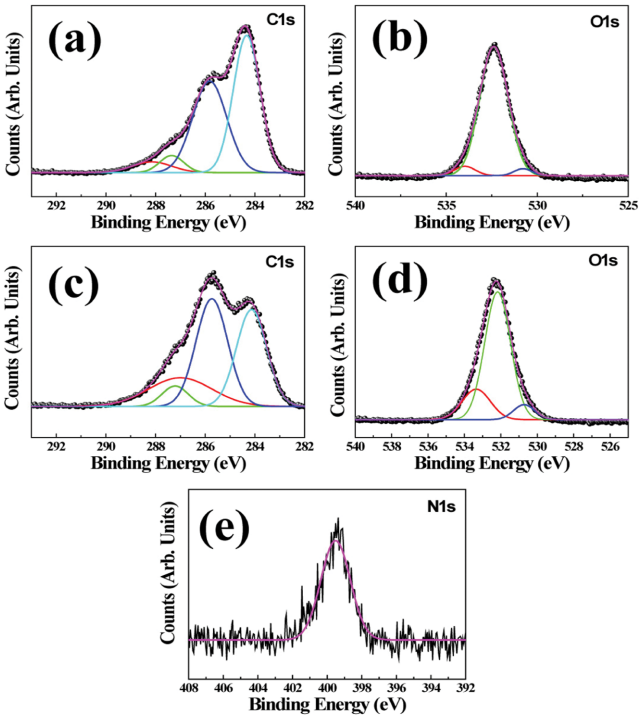

Figure 2. X-ray photoelectron spectroscopy (XPS) analysis of BCNWs (a) C1s; (b) O1s. XPS analysis of N-BCNWs: (c) C1s; (d) O1s; (e) N1s.

Table 1. C, O, and N Concentrations Calculated from XPS Spectra of the BCNWs and N-BCNWs Shown in Fig. 2

	BCNWs	N-BCNWs
C1s	75.16%	66.89%
O1s	24.82%	30.37%
N1s		2.74%

PEO/BCNWs and PEO/N-BCNWs at a concentration of 0.3 wt% were 0.67±0.23 and 0.59±0.10 μm (N=20), respectively, shown in Figure 3(b) and 3(c). At a concentration of 0.5 wt%, the diameters of electrospun PEO/BCNWs and PEO/N-BCMWs were 0.84±0.28 and 0.64±0.13 μm (N=20), respectively, shown in Figure 3(d) and 3(e).

The diameter of electrospun PEO/BCNWs was relatively larger due to the concentration of BCNWs (0.3 and 0.5 wt%) and presence of some thicker nanofibers. The diameter of the PEO/N-BCNWs, on other hand, was more uniform, also increased with a higher N-BCNWs concentration, but was on average slightly smaller than that of the PEO/BCNWs at the same concentration. Other researchers have reported previously that electrospun PEO with BCNWs at 0.2 and 0.4 wt% showed an increase in the fiber diameter according to the cellulose whisker concentration, which corresponded with enhanced mechanical properties.[10] Other studies fabricated PEO/CNC composite nanofibrous mats with homogeneous and heterogeneous microstructures due to the high concentrations of CNC.[11] In addition, we reported in our previous research that the diameter of composites of electrospun poly [(D,L-lactic)-*co*-(glycolic acid)] (PLGA) and amine plasma treated single-walled carbon nanotubes (*a*-SWCNTs) decreased compared to that of electrospun PLGA/untreated SWCNT because the surface energy of *a*-SWCNTs is larger than that of untreated SWCNTs, and the observed morphological differences affected the mechanical properties of the electrospun samples.[28] The morphological change of electrospun PEO/N-BCNWs compare to electrospun PEO/BCNWs showed a similar trend as in our previous our reports.

The internal structures of electrospun PEO incorporating BCNWs or N-BCNWs were investigated using HR-STEM, as shown in Figure 4. Compared to the BCNWs, the N-BCNWs were distributed more uniformly along the orientation of the nanofiber in the electrospun PEO.

The FTIR spectra of BCNWs and N-BCNWs are shown in Figure 5(a) and (b); the feature at wave-numbers 3338 cm^{-1} corresponds O-H stretching vibration, that at 2913 cm^{-1} to CH_2

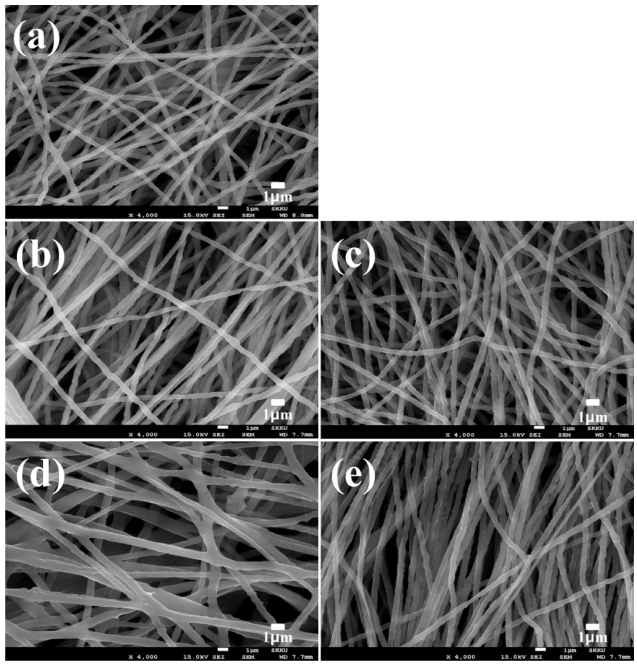

Figure 3. Field emission scanning electron microscopy (FE-SEM) images of electrospun (a) polyethylene oxide (PEO); (b) PEO/BCNWs (0.3 wt%); (c) PEO/N-BCNWs (0.3 wt%); (d) PEO/BCNWs (0.5 wt%); (e) PEO/N-BCNWs (0.5 wt%).

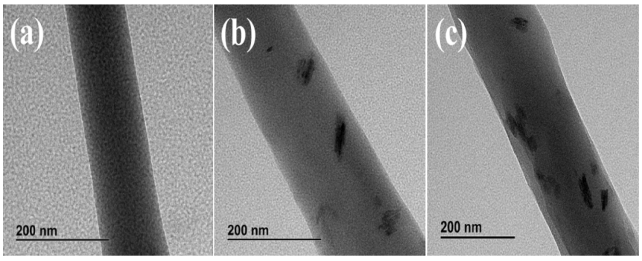

Figure 4. High-resolution scanning transmission electron microscopy images of electrospun (a) PEO; (b) PEO/BCNWs (0.3 wt%); (c) PEO/N-BCNWs (0.3 wt%).

stretching and those at 1427, 1335 and 1159 cm^{-1} to C-C stretching vibration. The peak 1107 cm^{-1} and 1054 cm^{-1} were assigned to skeletal/vibrations and ring vibrations, respectively. The peak of 1648 cm^{-1} indicates the deformation vibration of the absorbed water molecules.[30,31] The region around 1540 cm^{-1} for N-BCNWs indicates C-N stretching vibrations due to nitrogen functionalization.[32]

The FTIR spectra of electrospun PEO, PEO/BCNWs and PEO/N-BCNWs (0.3 and 0.5 wt%) are shown in Figure 5(c)-(g). The peaks of electrospun PEO were observed at 2883 cm^{-1} (CH_2 stretching), 1467 cm^{-1} (C-H bending mode), and 1341 cm^{-1} (CH_2 wagging). Other peaks were observed at 1279, 1240 and

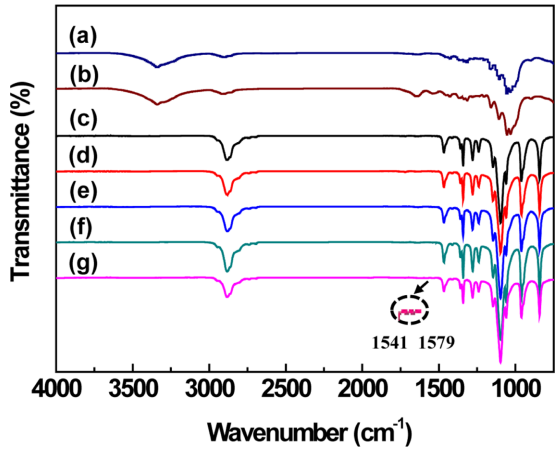

Figure 5. Fourier transform infrared spectra of (a) BCNWs; (b) N-BCNWs; electrospun of (c) PEO; (d) PEO/BCNWs (0.3 wt%); (e) PEO/N-BCNWs (0.3 wt%); (f) PEO/BCNWs (0.5 wt%); (g) PEO/N-BCNWs (0.5 wt%). The insert is the magnified image of amide II peaks.

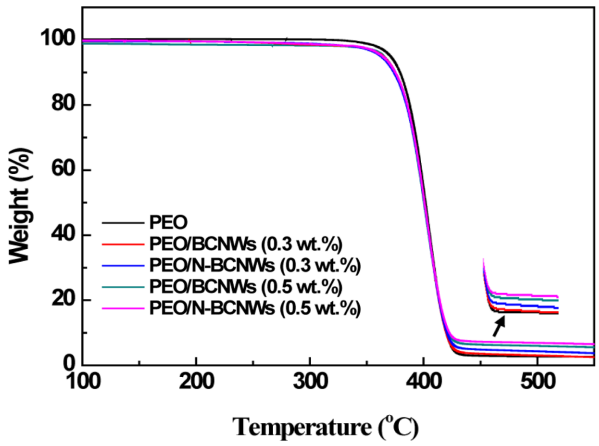

Figure 6. Thermogravimetric analysis (TGA) curves of weight as a function of measurement temperature of electrospun PEO, PEO/BCNWs, and PEO/N-BCNWs. The magnified image inserted over 430 °C (arrow).

1096 cm^{-1} (C-O-C stretching), 960 cm^{-1} (CH_2 wagging), and 841 cm^{-1} (C-O-C bending).[33] All composite nanofibers did not show any spectral changes compare to electrospun PEO due to the small concentration of BCNWs and N-BCNWs. However, weak peaks at 1541 and 1579 cm^{-1} for electrospun PEO/N-BCNWs could be identified as amide II peaks corresponding to the C-N stretching bond and in-plane N-H bend.[32]

Thermal Properties Evaluation of Electrospun PEO, PEO/BCNWs and PEO/N-BCNWs. The themal properties of the electrospun samples were measured using TGA and DSC. The TGA curves in Figure 6 show weight loss as a function of temperature. Similar to electrospun PEO, the composite nanofibers experienced almost no weight loss between 228 and 360 °C, and their decomposition temperature were observed at 430 °C. The total weight loss values for the electrospun PEO, PEO/BCNWs, and PEO/N-BCNWs are shown in Table 2. The weight loss of electrospun PEO/BCNWs and PEO/N-BCNWs was lower than electrospun PEO, and the residual amount of electrospun PEO/N-BCNWs was increased slightly about 1.4 and 1.5% at 0.3 and 0.5 wt% concentration, respectively, compared to electrospun PEO/BCNWs. This indicates that the thermal characteristics were enhanced by the improved chemical bonding between the N-BCNWs and the PEO polymer chains.

The DSC results in Figure 7(a) and (b) show the heat flow as a function of temperature for all electrospun samples, indicating the T_m and T_c values, respectively, by the peak positions. No glass transition temperature (T_g) peaks were observed. The T_m values under the second heating and T_c values under the

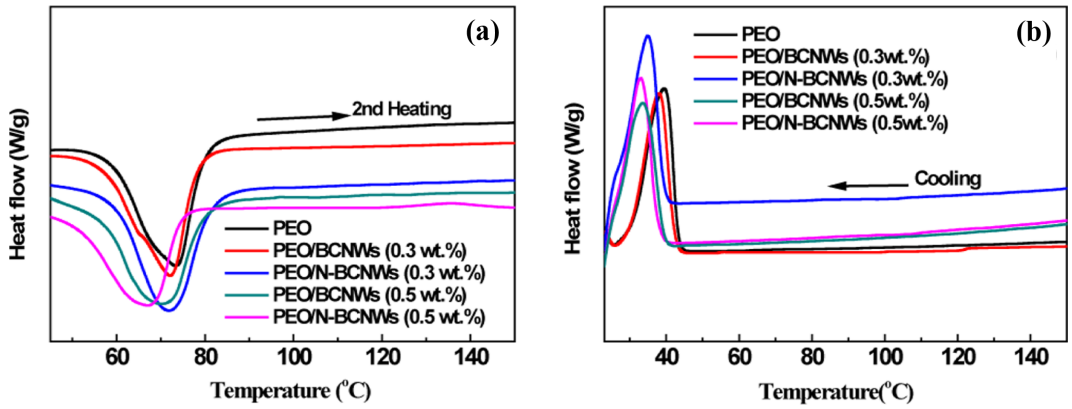

Figure 7. DSC thermograms as a function of measurement temperature of electrospun PEO, PEO/BCNWs, and PEO/N-BCNWs.

Table 2. Weight Loss, Melting Temperature (T_m), and Crystallization Temperature (T_c) Data Extracted from the TGA and DSC Curves

	Electrospun PEO	Electrospun PEO/BCNWs		Electrospun PEO/N-BCNWs	
		0.3 wt%	0.5 wt%	0.3 wt%	0.5 wt%
Weight loss(%)	97.17	96.08	95.44	94.37	92.89
T_m(°C)	73.78	72.26	71.81	70.10	67.70
T_c(°C)	39.33	38.35	35.03	33.24	32.97

cooling conditions for the electrospun PEO, PEO/BCNWs, and PEO/N-BCNWs are shown in Table 2. The T_m and T_c values of the electrospun PEO/N-BCNWs were slightly lower than those of the electrospun PEO and PEO/BCNWs at the same concentration. For both the PEO/BCNW and PEO/N-BCNW samples, the T_m and T_c values decreased with increasing concentration of cellulose nanowhiskers. Similar thermodynamical properties have been investigated for electrospun EVOH/BCNWs composite nanofibers[34] and electrospun PEO/CNC composite nanofibrous mats.[11] Those studies reported that when BCNWs and N-BCNWs were added as fillers, they interrupted the crystallization of PEO chains during the electrospinning process.[11,34]

Conclusions

The morphological, chemical, and thermal properties of electrospun PEO, PEO/BCNWs and PEO/N-BCNWs were investigated in order to understand the effects of BCNWs and N-BCNWs when incorporated within the polymer. BCNWs were cultured by *Gluconacetobacter xylium* and prepared by freeze drying. Nitrogen-functionalized BCNWs were successfully fabricated without inducing defects using N_2 plasma treatment in a microwave oven. The electrospun PEO, PEO/BCNW, and N-BCNW samples were fabricated with BCNW and N-BCNW concentrations of 0.3 and 0.5 wt% by electrospinning. The nitrogen groups on the surface of the N-BCNWs bonded with the hydroxyl groups in the PEO polymer, resulting in enhanced chemical bonding. The diameter of the electrospun PEO/N-BCNWs was slightly smaller than that of the PEO/BCNWs at the same concentration. The weight loss, T_m, and T_c values of electrospun PEO/BCNWs and PEO/N-BCNWs decreased with an increase in the concentration of nanowhiskers, and the values for the PEO/N-BCNWs were slightly smaller than those of the PEO/BCNWs at the same concentration. The ash content of nitrogen-containing samples after TGA confirmed the increased weight compare to other samples. The obtained results demonstrate that N-BCNWs used as a filler in PEO are suitable for various applications such as humidity sensor and biomedical fields.

Acknowledgements: This research was supported by the Basic Science Research Program through the National Research Foundation of Korea (NRF) under the auspices of the Ministry of Education (Grant No. 2009-0093817 and 2015R1C1A2A01056280) and by Nano·Material Technology Development Program through the National Research Foundation of Korea (NRF) funded by the Ministry of Science, ICT and Future Planning (2009-0082580).

References

1. K. Lej and G. Lewandowicz, *Polish J. Environ. Stud.*, **19**, 255 (2010).
2. Y. Zhao, Y. Qiu, H. Wang, Y. Chen, S. Jin, and S. Chen, *Int. J. Polym. Sci.*, **2016**, 1 (2016).
3. J. Kim, S.-Y. Choi, K. M. Kim, C. H. Lee, H. S. Park, S. S. Hwang, S. M. Hong, S. Kwak, and H.-O. Yoo, *Macromol. Symp.*, **245**, 565 (2006).
4. J. G. Archambault and J. L. Brash, *Colloids Surf. B: Biointerfaces*, **39**, 9 (2004).
5. M. K. Pilehrood, M. Dilamian, M. Mirian, H. Sadeghi-Aliabadi, L., P. Nousiainen, and A. Harlin, *Res. Int.*, **2014**, 1 (2014).
6. A. G. Supri1, M. D. S. Hajar, and M. P. M. Hanif, *Polym. Bull.*, **73**, 1 (2016).
7. S. K. Mahadeva and J. Kim, *Polym. Eng. Sci.*, **50**, 1199 (2010).
8. S. S. Jang and W. A. Goddard, *J. Phys. Chem. B,* **111**, 1729 (2007).
9. Haryanto, S. Kim, J. H. Kim, J. O. Kim, S. K. Ku, H. Cho, D. H. Han, and P. Huh, *Macromol. Res.*, **22**, 131 (2014).
10. W.-I. Park, M. Kang, H.-S. Kim, and H.-J. Jin, *Macromol. Symp.*, **249**, 289 (2007).
11. C. Zhou, R. Chu, R. Wu, and Q. Wu, *Biomacromolecules*, **12**, 2617 (2011).
12. D. Shi, F. Wang, T. Lan, Y. Zhang, and Z. Shao, *Cellulose*, **23**, 1899 (2016).
13. J. Wang, H. Jia, J. Zhang, L. Ding, Y. Huang, D. Sun, and X. Gong, *J. Mater. Sci.*, **49**, 6093 (2014).

14. E. R. P. Pinto, H. S. Barud, R. R. Silva, M. Palmieri, W. L. Polito, V. L. Calil, M. Cremona, S. J. L. Ribeiroa, and Y. Messaddeq, *J. Mater. Chem. C*, **3**, 11581 (2015).
15. Z. Abas, H. S. Kim, J. Kim, and J.-H. Kim, *Front. Mater.*, **1**, 1 (2014).
16. J. M. Dugan, J. E. Gough, and S. J. Eichhorn, *Nanomedicine.*, **8**, 297 (2013).
17. Z. Shi, Y. Zhang, G. O. Phillips, and G. Yang, *Food Hydrocolloid.*, **35**, 539 (2014).
18. M. M. Abeer, M. C. I. M. Amin, and C. Martin, *J. Pharm. Pharmacol.*, **66**, 1047 (2014).
19. S. Khan, M. Ul-Islam, W. A. Khattak, M. W. Ullah, and J. K. Park, *Carbohydr. Polym.*, **127**, 86 (2015).
20. C. Legnani, C. Vilani, V. L. Calil, H. S. Barud, W. G. Quirino, C. A. Achete, S. J. L. Ribeiro, and M. Cremona, *Thin Solid Films*, **517**, 1016 (2008).
21. M. U. Rani and K. A. A. Appaiah, *J. Food Sci. Technol.,* **50**, 755 (2013).
22. B. S. Hungund and S. G. Gupta, *J. Microbiol. Biotechnol.,* **2**, 127 (2010).
23. L. Fu, J. Zhang, and G. Yang, *Carbohydr. Polym*., **92**, 1432 (2013).
24. M. Martinez-Sanz, A. Lopez-Rubio, and J. M. Lagaron, *Carbohydr. Polym*., **85**, 228 (2011).
25. R. A. N. Pertile, F. K. Andrade, C. Alves Juniorr, and M. Gama, *Carbohydr. Polym*., **82**, 692 (2010).
26. O. J. Yoon, C. Y. Jung, I. Y. Sohn, H. J. Kim, B. Hong, M. S. Jhon, and N.-E. Lee, *Compos. Part A Appl. S*., **42**, 1978 (2011).
27. F. Esa, S. M. Tasirin, and N. A. Rahman, *Agric. Agric. Sci. Procedia*, **2**, 113 (2014).
28. O. J. Yoon, H. W. Kim, D. J. Kim, H. J. Lee, J. Y. Yun, Y. H. Noh, D. Y. Lee, D. H. Kim, S. S. Kim, and N.-E. Lee, *Plasma Process. Polym*., **6**, 101 (2009).
29. C. Huang, Q. Yang, and S. Wang, *Asian J. Chem*., **24**, 5476 (2012).
30. D. Li, K. Ao, Q. Wang, P. Lv, and Q. Wei, *Molecules*, **21**, 618 (2016).
31. J. George, K. V. Ramana, A. S. Bawa, and Siddaramaiah, *Int. J. Biol. Macromolec*., **48**, 50 (2011).
32. C. Choi, J.-H. Ahn, G.-W. Jeong, H.-S. Lee, S.-J. Choi, W.-S. Kim, and J.-W. Nah, *Polym. Korea*, **40**, 643 (2016).
33. I. Pucic and T. Jurkin, *Radiat. Phys. Chem*., **81**, 1426 (2012).
34. M. Martínez-Sanz, R. T. Olsson, A. Lopez-Rubio, and J. M. Lagaron, *Cellulose,* **18**, 335 (2011).